

HD 98800: A most unusual debris disc

P. E. Verrier^{1*} and N. W. Evans^{1*}

¹*Institute of Astronomy, University of Cambridge, Madingley Road, Cambridge, CB3 0HA, United Kingdom*

8 July 2008

ABSTRACT

The dynamics of planetesimals in the circumbinary debris disc of the quadruple star system HD 98800 are investigated. Evolving a spherical shell of test particles from a million years ago to the present day indicates that both coplanar and retrograde warped discs could exist, as well as a high inclination halo of material. Significant gaps are seen in the discs, as well as unexpected regions of stability due to the retrograde nature of the stellar orbits. Despite a viewing angle almost perpendicular to the direction of the warp of the planetesimal disc it is still intersected by the line of sight for eccentricities of the outer orbit of 0.5 or less.

Key words: celestial mechanics – planetary systems – methods: *N*-body simulations – stars: individual: HD 98800

1 INTRODUCTION

HD 98800 is an interesting and unusual system of four 10 Myr old post T-Tauri K stars – two spectroscopic binaries A and B in orbit about one another – located in the TW Hydrae association (Torres et al. 1995, Kastner et al. 1997). It has a large infrared excess attributed to a circumbinary disc around the B pair (Koerner et al. 2000; Prato et al. 2001; Furlan et al. 2007). Substantial extinction towards this pair is evidence that they are observed through some of this material (Soderblom et al. 1998, Tokovinin 1999). A photometric variability is also seen, but with no definite period (Soderblom et al. 1998). Both the apparent absence of CO molecular gas in the disc (Dent et al. 2005) and infrared spectrum modelling indicate that this is a T-Tauri transition disc that is just reaching the debris disc stage, with a collisional cascade having been recently initiated (Furlan et al. 2007; Wyatt et al. 2007). The orbits of stars are all highly eccentric and inclined, creating a dynamical environment unlike almost all other known debris discs (Tokovinin 1999; Prato et al. 2001).

The dust disc here is generally agreed to be an annulus around the B binary, but the exact structure varies from model to model. Koerner et al. (2000) estimate a coplanar narrow ring outwards of about 5.0 ± 2.5 au from the two stars, themselves separated by approximately 1 au. Prato et al. (2001) however determine a 1 au high coplanar ring now from 2 and 5 au. Boden et al. (2005) argue that the line of sight extinction means that the disc is not coplanar with the sub-binary unless it is very flared. Furlan et al. (2007) suggest an inner optically thin ring at 2 au and an outer puffed up optically thick wall 0.75 au high at 5.9 au, with a gap between the two. Recently, Akeson et al. (2007) showed that a single continuous physically and optically thick coplanar disc between 3 and 10 au can reproduce the observed spectral energy distribution. To explain the extinction, they used dynamical models of test particles to

show that the inclined stellar orbits could create a warp in the dust disc, the outer layers of which could then just intercept the line of sight.

The unusually large infrared excess has been argued by Lagrange et al. (2000) to be caused by one of four reasons. The first is that a dust avalanche is currently in progress. Radiation pressure acts to push dust grains outwards. When the disc is very dusty, these can impact other dust grains, creating more particles that are themselves pushed outwards, colliding and creating yet more dust, and so on. The second possibility is there is undetected gas maintaining the dust population against radiation pressure. The third and fourth reasons are applicable when the wide orbit has an eccentricity of near unity, much higher than currently believed. In this case, it is possible that either an encounter with the A pair has heated the outer edges of the disc, resulting in abnormally high infrared radiation, or disrupted a Kupier Belt-like structure, resulting in collisions and releasing large amounts of dust. As the eccentricity is now known to be much lower, these two possibilities are less likely, although it should be noted that the wide orbit is currently very near to periastron.

The first two possibilities present difficulties in modelling the system. If the system is undergoing a dust avalanche or is gas-rich, then radiation pressure, collisions and gas dynamics must be included. For example, Wyatt et al. (2007) has calculated the dust collision timescale to very short (0.36 years), so collisional effects are important in modelling the dust evolution. However, in debris discs, dust is generated from an underlying planetesimal population, usually through a collisional cascade. In this case, the dust population follows the planetesimal population, which is less complex to model. If the disc has large amounts of gas or a dust avalanche is occurring, this may, of course, no longer be the case. Models of the planetesimal population remain interesting though, especially in such an unusual stellar environment. Indeed, the high inclination and eccentricities suggest that little stability is likely, yet some must exist. Constraining possible planetesimal locations and then

* E-mail: pverrier@ast.cam.ac.uk (PEV); nwe@ast.cam.ac.uk (NWE)

comparing with observations of the dust location may even be able to distinguish between the possible scenarios above. They would also serve as an indication of whether any planetary stability might be possible in this system.

There is one other debris disc known in a similar stellar system to HD 98800. This is GG Tau, which has a circumbinary debris disc of several hundred au radius in a quadruple star system with the same hierarchy (Guilloteau et al. 1999). However, in this case the stars are about ten times more distant, the mass ratios much smaller and their orbits relatively coplanar so more stability would be expected (Beust & Dutrey 2005, 2006). Dynamical modelling has shown that the circumbinary material forms a sharp ring and a more diffuse disc component.

HD 98800 remains an unusual environment, and the high inclination and eccentricity of the stellar orbits will have a significant effect on the dynamics and structure of the planetesimal population of the debris disc. This effect has yet to be studied in detail, and is investigated here using direct numerical integrations. Section 2 gives a description of the stellar system and the simulation parameters. The results are then presented in Section 3 and conclusions given in Section 4.

2 METHOD

2.1 The Stellar System

The wide orbit of the sub-binaries A and B is reasonably determined, as is that of the stars Ba and Bb in the B stellar pair. However the orbit of the other pair, Aa and Ab, is only partly known as the smaller star is not resolved. The parameters for all three orbits are listed in Table 1 and shown in Figure 1.

Tokovinin (1999) derives three possible fits to the wide orbit, fixing the eccentricity in each case as 0.3, 0.5 and 0.6 and assuming a total system mass of $2.6 M_{\odot}$. Table 1 shows the 0.5 eccentricity case, and Table 2 shows the others. Apart from the period (and hence separation), the orbital parameters do not vary much between the different solutions.

The A pair is a single-lined spectroscopic binary so only a partial radial velocity orbit has been determined (Torres et al. 1995). Prato et al. (2001) use evolutionary tracks to estimate the mass of the Aa star as $1.1 \pm 0.1 M_{\odot}$. The orbital inclination is not known, but the mass and separation of Ab can be found as a function of this parameter, as shown in Table 3. A wide range of inclinations are still possible even given the constraint that the star is small and unobservable. It is likely that this small star is unimportant to the dynamics of the circumbinary disc, and so the sub-binary can be modelled as a single object. However, it might alter the dynamics of the stellar orbits, and this is investigated in the next sub-section.

2.2 The Stellar Dynamics

The mutual inclination for the stellar orbits given in Table 1 can be calculated using the formula

$$\cos \phi = \cos i_1 \cos i_2 + \sin i_1 \sin i_2 \cos(\Omega_2 - \Omega_1) \quad (1)$$

where Ω_j are the longitudes of ascending node, i_j are the inclinations relative to a given reference plane and ϕ is the mutual inclination, the angle between the angular momentum vectors of the two orbits (see e.g. Smart 1953). It is found to be in this case 143.7° , and is similar for the other two orbits (see Table 2). Notably, it is retrograde.

Table 1. The orbital and physical parameters for the stellar system HD 98800. The wide orbit of AB is fit II from Tokovinin (1999), with the semi-major axis calculated assuming a total system mass of $2.6 M_{\odot}$ and the MJD taken from the middle of the year 2025 given as the time of periastron of the AB pair. The Bab pair orbit is taken from the joint-fit given by Boden et al. (2005). The orbit of the A sub-binary is from Torres et al. (1995). Note that the reference plane is that perpendicular to the line of sight and the longitudes of the ascending nodes are measured from North through East.

Orbital Parameter	Wide	A sub-binary		B sub-binary	
	A	Aa	Ab	Ba	Bb
Mass (M_{\odot})	–	1.1 ± 0.1		0.699 ± 0.064	0.582 ± 0.051
Radius (R_{\odot})	–			1.09 ± 0.14	0.85 ± 0.11
a (au)	67.6			0.447 ± 0.013	0.536 ± 0.013
Period	345 yr	262.15 ± 0.51 d		314.327 ± 0.028 d	
e	0.5	0.484 ± 0.020		0.7849 ± 0.0053	
i ($^{\circ}$)	88.3			66.8 ± 3.2	
ω ($^{\circ}$)	224.6	64.4 ± 2.1		289.6 ± 1.1	
Ω ($^{\circ}$)	184.8			337.6 ± 2.4	
τ (MJD)	60840	8737.1 ± 1.6		52481.34 ± 0.028	

Table 2. The three different orbital fits for the wide orbit AB from Tokovinin (1999). Here ϕ is the mutual inclination to the orbit of the B stellar pair.

Orbital Parameter	Orbit		
	I	II	III
a (au)	61.9	67.6	78.6
Period (years)	302	345	429
e	0.3	0.5	0.6
i ($^{\circ}$)	87.4	88.3	88.7
ω ($^{\circ}$)	210.7	224.6	224.0
Ω ($^{\circ}$)	184.8	184.8	184.8
τ (MJD)	59379	60840	61205
ϕ ($^{\circ}$)	143.0	143.7	143.9

As mentioned, it is likely for an investigation of the dynamics of the circumbinary disc that the Aab system can be reasonably approximated by a single star of mass $1.3 M_{\odot}$, consistent with the minimum mass of Ab and the total system mass assumed by Tokovinin (1999). In this case, the system becomes a hierarchical triple and can be numerically studied using the MOIRAI code (Verrier & Evans 2007). A million year simulation of orbit II in this case is shown in Figure 2. Energy is conserved to a relative error of 10^{-7} and the integration was checked with a standard Bulirsch-Stoer integrator (Press et al. 1989) and found to be in agreement. The semimajor axes of the stars and the wide orbit's eccentricity are not shown, as they remain constant through out the simulation. Interestingly, the system is currently near its maximum eccentricity and mutual inclination. For all three possible outer orbits, the eccentricity and mutual inclination vary smoothly in a secular manner, with maximum angular separation between the orbital planes occurring for minimum eccentricity of the inner orbit. The amplitude of the variation is very similar in all cases and the periods are 65, 60 and 75 Kyr for orbits I, II and III respectively. In fact the system remains in this stable configuration for at least a Gyr, as well as to at least 10 Myr ago.

The orbital behaviour is well described by the octupole secular theory of Ford et al. (2000), as overplotted in Figure 2. This theory uses a third order expansion of the systems Hamiltonian in the ratio

Table 3. The mass of star Ab and the A binary's semimajor axes as a function of inclination to the plane of the sky.

Inclination ($^{\circ}$)	90	70	60	50	40	30	20	10
M_{Ab} (M_{\odot})	0.22	0.23	0.25	0.29	0.36	0.49	0.80	2.36
a (au)	0.88	0.88	0.89	0.89	0.91	0.94	0.99	1.21

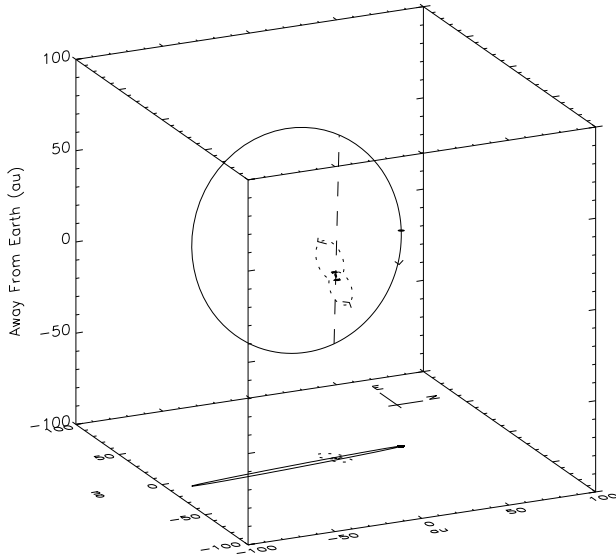


Figure 1. The physical orbit of the quadruple star system HD 98800 in three dimensions. The wide orbit is fit II from Tokovinin (1999) and the B pair orbit that of Boden et al. (2005). Units are in au, and the plot is centred on the barycentre of the B stellar pair. A projection of the orbits onto the plane of the sky is also plotted along with the relevant directions. The B pair orbit is overplotted magnified 20 times as dotted lines. The position of stars at the epoch MJD 52481.34 (mid 2002, inner orbit at periastron) and the direction of the orbits are given. Finally, the line of intersection of the two orbits is also plotted as a dashed line.

of the semimajor axes of the stellar orbits to obtain a set of coupled first order differential equations, their equations (29) to (32), for the time variation of the eccentricities and arguments of periastron of the inner and outer orbits that can be numerically solved. The inclination and nodes of the system are then derivable from these elements, and the semimajor axes remain constant. From the figure, it can be seen that the theory is in excellent agreement with the results from the full equations of motion, with only a small phase drift after a Myr. In fact, because the two orbits are fairly separated a quadrupole level theory is sufficient to describe the system. In this approximation the outer eccentricity is a constant, as seen here. Thus, in the three body approximation the stars follow a stable secular evolution and can be accurately integrated by the MOIRAI code.

The full four body system can now be considered. The mass of Ab and the semimajor axis of the orbit can only be resolved by assuming the inclination to the line of sight (see Table 3). The longitude of ascending node of the orbit remains an unknown, but is needed to constrain the mutual inclination of the orbital planes. Therefore, to investigate possible dynamics, a set of simulations were run for inclinations in the range 90° to 30° (shown in Table 3) with values of ascending node ranging from 0° to 315° in 45° steps and using wide orbit II. To do this, the fourth star was approximated as a planet around its primary, Aa, in the MOIRAI code.

In all cases, there is little difference to the three body results. An example is shown in Figure 3. The only change is to the secular period of orbit Ba-Bb together with a slight modulation of their minimum eccentricity, and in some cases even this does not occur. A slight change in the period of the secular variations is un-

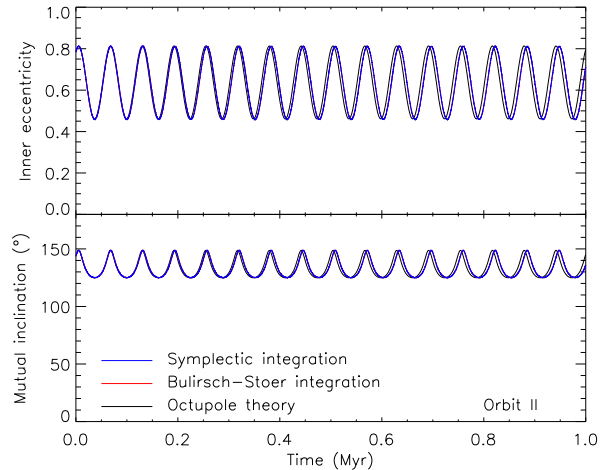


Figure 2. The three body stellar orbital evolution for orbit II over 1 Myr from numerical and theoretical modelling. The blue line shows the results from the symplectic integrator, identical to those from the Bulirsch-Stoer shown in red. The octupole theory results are shown in black, and differ only slightly in phase. The semimajor axes of both orbits and eccentricity of the outer orbit are constant and not shown.

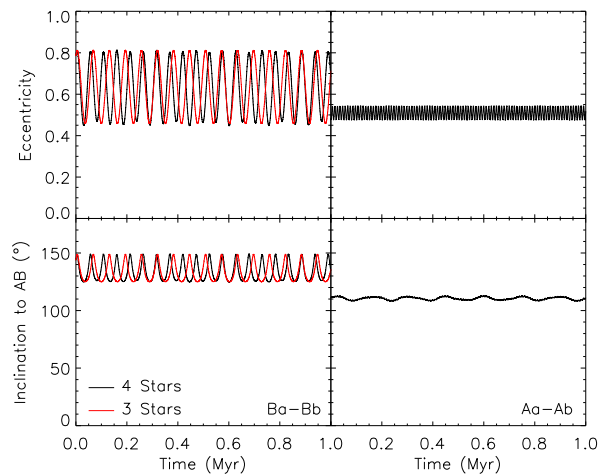


Figure 3. The evolution of the stellar orbits for the four body case with $i_{Ab} = 30^\circ$ (relative to the plane of the sky) and $\Omega_{Ab} = 45^\circ$ compared to the three body approximation. The left hand panels show the orbit of the inner binary Ba-Bb, red indicating the three body approximation and black the four body case. The right panels show the evolution of the orbit of the Aa-Ab binary. The eccentricity of the wide binary A-B once again remains effectively constant, as do the semimajor axes of all orbits.

likely to alter the overall structure of the planetesimal disc. Indeed, Beust & Dutrey (2006) also find that modelling the distant sub-binary in GG Tau as a single object has little effect on the disc structure there. Hence, the three body approximation is a reasonable assumption and will be used for the purposes of this investigation.

2.3 Other Physics

As the disc mass is low ($0.002M_{\oplus}$, Prato et al. 2001), it is reasonable to model the planetesimals as non-interacting test particles. However, there is one interaction process that may be important in

the modelling of the planetesimals, namely collisions. Following Wyatt et al. (2007), it is possible to estimate the collision timescale from the observed infrared excess. Although this assumes a collisional cascade is underway, it should provide a lower limit to the timescale if dust is in fact maintained by gas or generated in an avalanche. The collision timescale is given by their equation (13) as

$$t_c = \left(\frac{3.8\rho r^{2.5} dr D_c}{M_*^{0.5} M_{tot}} \right) \left(\frac{(12q - 20)(1 + 1.25(e/I)^2)^{-0.5}}{(18 - 9q)G(q, X_c)} \right) \quad (2)$$

where q is assumed to be 11/6 for a collisional cascade and G is a function of q and $X_c = D_{cc}/D_c$, D_c being the diameter of largest planetesimal in the cascade, taken as 2000 km, and D_{cc} being the smallest planetesimal that has enough energy to destroy another of size D_c . ρ is the planetesimal density and taken as 2700 kg m^{-3} , r is the planetesimal belt radius in au, dr is the planetesimal belt width in au, M_{tot} is the total mass of material in the cascade in M_\oplus , e is the mean orbital eccentricity of planetesimals and I is the mean orbital inclination of planetesimals in radians. The factor $G(q, X_c)$ is given by their equation (9) as

$$G(q, X_c) = (X_c^{5-3q} - 1) + \frac{6q - 10}{3q - 4} (X_c^{4-3q} - 1) + \frac{3q - 5}{3q - 3} (X_c^{3-3q} - 1) \quad (3)$$

and X_c by their equation (11) as

$$X_c = 1.3 \times 10^{-3} (Q_D^* r M_*^{-1} f(e, I)^{-2})^{1/3} \quad (4)$$

where $f(e, I)$ is the ratio of the relative collision velocity to the Keplerian velocity and taken as 0.1 and Q_D^* is the dispersal threshold which is the specific incident energy needed to destroy a particle, assumed to be 200 J kg^{-1} . In addition, it is also assumed that $e \approx I$.

The two stars Ba and Bb are approximated as a single object of mass and luminosity as $1.57 M_\odot$ and $0.58 L_\odot$ respectively (Prato et al. 2001). The total mass of the disc can be calculated from equations (4) to (6) of Wyatt et al. (2007) as

$$M_{tot} = 5.194 \sigma_{tot} = 14.36 r^2 \quad (5)$$

and hence the collision timescale as a function of r and dr is

$$t_c = 1.014 \times 10^6 r^{0.5} dr \frac{1}{G(q, X_c)} \quad (6)$$

The exact extent of the planetesimal disc is as yet unknown, but the location of the dust can be used as an approximation. The minimum radius for dust to be able to exist is given as 2.2 au by Low et al. (2005), but Koerner et al. (2000) estimates the disc to be between 5.0 and 18 au. In the first case of a wide disc around 2 au, the collision timescale is 30 Kyr, and in the second case of a disc from 5 to 18 au, it is 200 Kyr. Preliminary results from test simulations indicated that the disc must lie further out than 2 au, so the higher timescale is applicable and gravitational effects will dominate the behaviour of the planetesimals here. Thus, for the purpose of determining overall disc structure, no additional physics needs to be included.

2.4 Method of investigation

To summarise, the stars are modelled as a three body system with a disc of massless planetesimals interacting through gravitational effects with the stars only. The three possible orbital configurations for the wide binary will all be considered. To model the disc, the MOIRAI code has been shown to be accurate, and the test particle

Table 4. The test particle grid used in the simulations.

Orbital Parameter	Min	Max	Step Size
a (au)	1.75	33.85	0.1
e	0.0	0.04	0.02
i ($^\circ$)	0	180	5
ω ($^\circ$)	0	240	120
Ω ($^\circ$)	0	240	120
M ($^\circ$)	0	240	120
N_{tp}	965034		

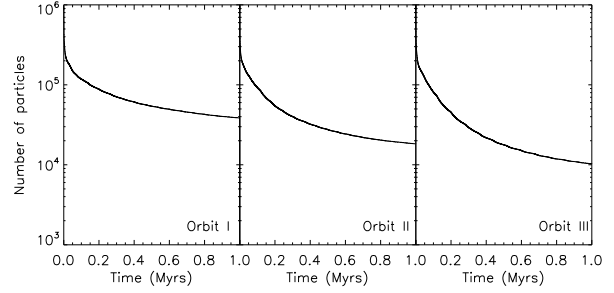


Figure 4. The test particle decay rates for the three simulations. The half-life (ignoring the first 0.1 Myr when all initially unstable particles are removed) is about 0.3 Myr for orbit I, 0.2 Myr for orbit II and 0.1 Myr for orbit III.

disc can be implemented as circumbinary particles around the B stellar pair.

The models discussed in the introduction have all assumed that the disc is coplanar with the B binary, but there is evidence for inclined discs around similar multiple stars. For example, the close binary pair in the T Tauri system were recently determined to have misaligned circumstellar discs (Skemer et al. 2007), and polarization surveys have found a small number of similar cases (Monin et al. 2006). Because of this, the test particle distribution is not initially taken as coplanar. Instead, they are spaced uniformly in inclination and longitude relative to the B binary pair. The initial surface density of the disc is taken as $1/r$ and the grid of test particles runs from 1.75 au to 33.85 au (inner binaries radius to half the outer binaries radius), as shown in Table 4. As the present day configuration, stability and geometry of the system are of interest to compare to observations, the simulations are run from 1 Myr ago to present day (defined as the periastron time of the Ba-Bb pair from Table 1). The results from these simulations are presented in the next section.

3 RESULTS

The stability of planetesimals is indicated by the stability of the test particles. These are removed from the simulation if they cross either of the stellar orbits or if they become unbound. The test particle decay rates are shown in Figure 4 for the three different simulations. The half-life is short and by the end of the simulations the decay rate has levelled out, although some particles are still being slowly eroded from very unstable locations. The majority of unstable particles are removed on 10 to 100 Kyr timescales as they become unbound or cross the outer orbit. If the simulations are run for an additional million years, there is no further significant loss of particles so the simulation length is sufficient to determine the system state, especially given the system age of about 10 Myr.

The final structure at the end of the simulation is similar in

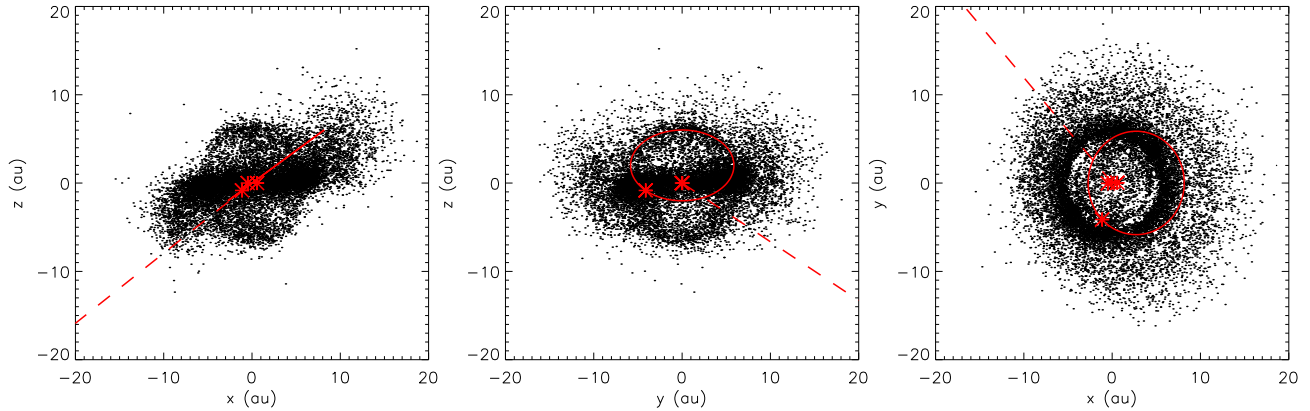


Figure 5. Edge and face on views of the circumbinary material for the simulation using orbit II. The inner binary’s orbit lies in the $z = 0$ plane and the line of intersection with the outer stellar orbit is along the y -axis. The orbits of the stars and their current positions are overplotted in red, but the wide orbit is shown at a tenth of its actual size. The line of sight is also shown as a dashed line.

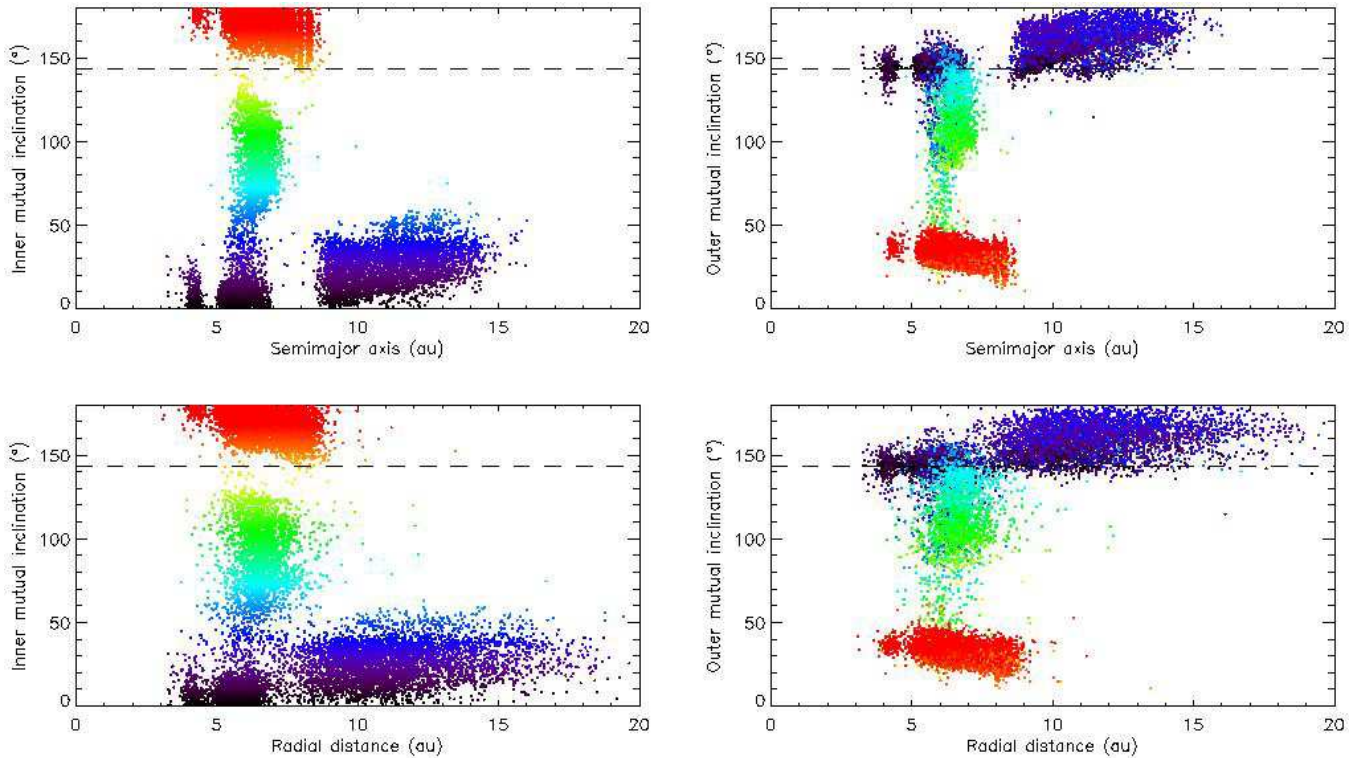


Figure 6. The final test particle distributions for the simulation using orbit II. The two panels on the left show the inclination relative to the inner binary as a function of semimajor axis and radial distance from the center of the binary, with colour indicating inner mutual inclination as shown. The two panels on the right show the inclination relative to the wide orbit, but the colour still indicates inner inclination. Overplotted as a dashed line is the mutual inclination of the two stellar orbits.

all three orbital cases, and is well illustrated by the case of orbit II. Shown in Figure 5 is the spatial distribution of the circumbinary material. A warped coplanar disc is apparent around the inner binary, as well as a large amount of higher inclination material. The disc appears to have a small inner ring separate to the main bulk of particles. There is also a slight clumping of material apparent, perpendicular to the inner orbits line of apses. The high inclination material appears to form another ring or halo perpendicular to the disc, most obvious in the middle plot of the figure.

These different structures are more clearly seen in a plot of

inclination as a function of distance from the inner binary, as shown in Figure 6. Here, the particle distribution relative to the inner and outer orbits is plotted for both radial distance and semimajor axis. To identify different populations, particles are colour coded to their inclination relative to the inner binary’s orbit.

Three distinct features are seen in these plots: a prograde coplanar disc with two gaps; a retrograde disc with one gap and an extended ring or halo, as seen in the spatial plot, from 50° to 130° inner inclination. These populations are well separated in in-

clination by two gaps around 50° and 140° , the later being centred on the inclination of the outer binary's orbit.

The coplanar disc extends from about 4 to 15 au, with two gaps between 4.5 and 5 au (seen very clearly in Fig. 5) and 7 and 8 au. The gaps are less obvious in the radial distribution due to particle eccentricity, but are still apparent. The outer regions of this disc are inclined up to almost 50° and provide the warped material seen in the spatial plot. There is also a series of breaks in the semimajor axis distribution slightly apparent both here and in the retrograde disc (these are very clear in Figure 9), presumably due to resonant features as they are much larger than the grid resolution of 0.1 au. Relative to the outer orbit, the disc material in the outer warped regions is perturbed up to almost completely retrograde orbits, explaining its stability.

The retrograde (relative to the inner binary) disc is smaller, extending from 4 to 9 au, but also has a gap between 4.5 and 5 au. The outer regions here are perturbed towards the same inclination as the outer orbit, similar but opposite to the coplanar disc's structure. This disc is in fact much sharper relative to the outer star, where it is prograde with an inclination of around 30° .

The last component is the halo-like structure. This extends only from 5.0 to 8.0 au but covers a large range of inclinations relative to both stellar orbits. This material is unusual in remaining stable at very high inclinations, but similar stable high inclination particles have been seen before by Beust & Dutrey (2006) in simulations of GG Tau.

These three separate populations are also very distinct in a plot of final versus initial inclination, as shown in Figure 7. Particles in the prograde disc start with initial inner inclinations in the range 0° to 50° and remain within that range. Those in the halo, starting in the range 60° to 125° , also remain there although there is less variation in the middle of this group. Finally, the retrograde disc is clearly confined by the inclination of the outer stellar orbit, and particles here start and remain in the range 145° to 180° . These populations are again clear in the outer inclination distribution, as can be seen from the colour coding of the particles. There is in fact a fourth diffuse population visible here, at around 70° to 90° , which forms a more diffuse ring at a different angle to that of the main halo.

The initial outer inclination distribution is different for the orbit I and III simulations, as the stars start in slightly different places. However, the components evolve to the same final inclination distribution, showing that the results are robust and do not strongly depend on parameters such as the initial longitudes. Note also that in the orbit II case no particles start with initial outer inclinations less than about 30° , so it could be possible that another region of stability exists here. However, a disc of particles started coplanar with this outer orbit very rapidly became unstable, with no material surviving to the end of the simulation.

A radial profile of the three main structures can be plotted by using the inner inclination range to characterise them. This is shown in Figure 8 for each simulation. The coplanar disc (black) is defined as starting between 0° to 50° , the halo (green) between 55° to 140° and the retrograde disc between 145° to 180° . In each case the profiles of each component are very different, and the gaps in the two disc very apparent.

The radial profiles here are the result of the evolution of an initial $1/r$ distribution. A simulation was rerun for a flat initial density profile in the orbit II case. The resulting disc profiles were similar, although the inner and outer edges were slightly steeper. The profile of the halo also remained largely unchanged.

The most notable difference between the three simulations is

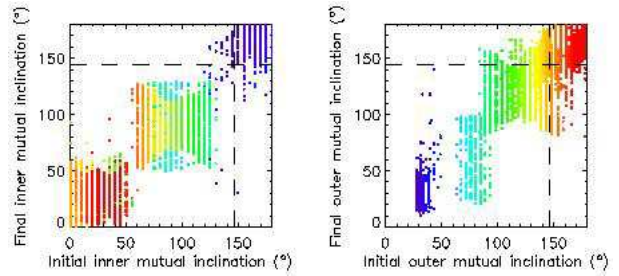


Figure 7. The initial test particle inclinations related to their final inclinations for the simulation using orbit II. The left panel shows inclination relative to the inner binary and the right panel relative to the outer wide orbit. Colour now indicates initial outer inclination to highlight the small population around 80° in the right hand plot. The dotted vertical line shows the initial mutual stellar inclination and the horizontal the final.

the generally greater stability in the lower eccentricity cases and the existence of an extended retrograde disc in the orbit I case. This stability is shown in greater detail in Figure 9, and compared to the other simulations. As the extended prograde coplanar disc is retrograde relative to the outer star, this disc is prograde to it. The extended prograde disc is itself less populated here, but both features can partly be explained by the initial particle inclinations. The stellar orbits are different here and particles that are retrograde relative to the inner star are more coplanar with the outer star than in the other orbital cases, and those that have prograde inner inclinations have lower outer inclinations. Thus, fewer particles start in the prograde extended disc, while more start in the retrograde case. It should be noted, however, that even if the initial inclination distribution is similar to the other two simulations, a retrograde extended disc is still seen. The eccentricity of the stellar orbits is therefore still likely to be important to these features, as can be seen by the decreasing radial extent of the prograde disc from orbit I to III in Figure 9. Indeed, as discussed above, a retrograde disc relative to the outer star for the orbit II case is completely unstable.

The radial extent of the structures seen in the three simulations is detailed in Table 5 and compared to both previous estimates of the size of the observed dust disc and empirical stability limits from numerical studies of general binary and triple systems. These empirical limits show the inner and outer radius for coplanar circumbinary stability by modelling the stars as a low inclination triple system (Verrier & Evans 2007) and as two coplanar decoupled binary systems (Holman & Wiegert 1999). A more general result from Verrier & Evans (2007) is that in cases of high stellar eccentricity and mass ratio the stable region was more complex than a completely stable ring, with gaps appearing that were most likely due to overlapping resonances from the two stellar orbits, as seen here. The extended outer regions of the prograde and retrograde discs are outside the empirically predicted stable region. This is most likely an effect due to the high inclinations and the particles retrograde nature relative to the outer or inner orbit, as retrograde orbits are generally more stable than prograde. However, the inner edges are well predicted.

An important feature of the observations of the system is the extinction and photometric variability towards the B binary, attributed to disc material along the line of sight by Tokovinin (1999) and Boden et al. (2005). Akesson et al. (2007) find that for the system they investigate the line of sight can just intercept the top of a warped disc of test particles. To see what material, if any, occurs along the line of sight here, we plot the azimuthal structure of the disc, as shown in Figures 10 and 11 for the case of orbit II. Here,

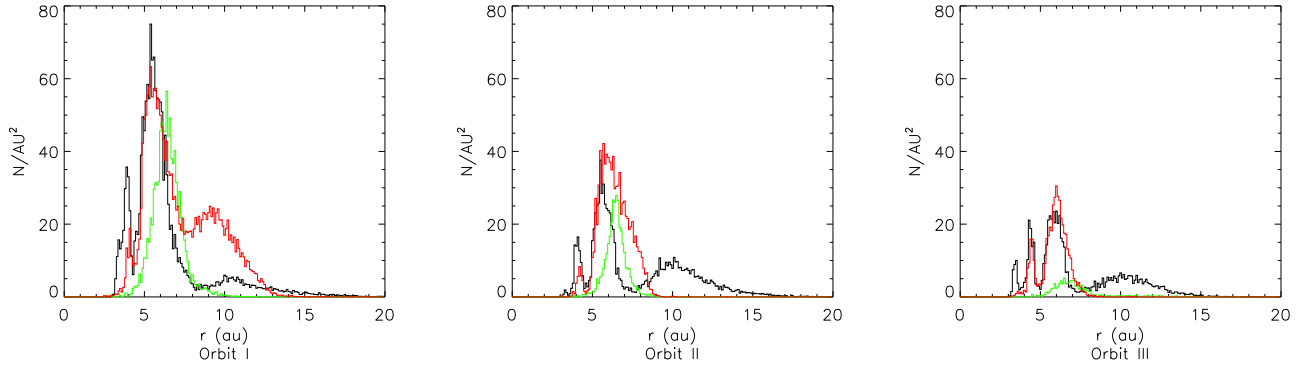


Figure 8. The radial profile of the three inclination components of the circumbinary material for all three simulations, showing the surface density as a function of radius. The coplanar disc is plotted in black, the halo in green and the retrograde disc in red. Note that for the orbit I case the retrograde disc starts at 105° instead of 145° due to the differences in the initial inclinations of the stars for this orbit. The retrograde disc and halo here also now overlap in inner inclination, and are separated using their outer inclination instead.

Table 5. The radial extent of the disc around HD 98800 B. The top four rows show other models of this system, the rest show empirical fits from general binary and triple systems and the extent of the three different inclination components for each possible outer orbit from the simulations here.

Model	Inner edge (au)	Outer edge (au)
Koerner et al. (2000)		5.0 ± 2.5
Prato et al. (2001)	2.0	5.0
Furlan et al. (2007)	2.0	gap 5.9
Akeson et al. (2007)	3.0	10.0
Orbit I		
Holman & Wiegert (1999)	4.1	10.9
Verrier & Evans (2007)	3.9	11.0
Disc	3.0 – 4.0	gap 4.5 – 8.0 gap 9.0 – 20.0
Halo	5.0	8.0
Retrograde	3.5 – 4.0	gap 4.5 – 7.0 gap 7.5 – 13.0
Orbit II		
Holman & Wiegert (1999)	4.1	4.3
Verrier & Evans (2007)	3.9	0.6
Disc	4.0 – 4.5	gap 5.0 – 7.0 gap 8.0 – 15.0
Halo	5.0	8.0
Retrograde	4.0 – 4.5	gap 5.0 – 9.0
Orbit III		
Holman & Wiegert (1999)	4.1	7.0
Verrier & Evans (2007)	3.9	7.3
Disc	3.0 – 3.5	gap 4.0 – 4.5 gap 5.0 – 7.0 gap 8.0 – 15.0
Halo	5.0	8.0
Retrograde	4.0 – 4.5	gap 5.0 – 8.0

the system has been rotated so that the inner binary lies in the horizontal plane with its periastron at an azimuthal angle of 0° . Each panel then shows the height above the plane as a function of radial distance within the plane of the inner binary in segments of 10° in azimuthal angle. Particles are colour coded to inner mutual inclination as for Figure 6 to distinguish the different components. The locations of the three stars are also shown (the position of the outer star is shown reduced by a factor of ten), as is the line of sight on the relevant plot.

The warp in the prograde disc is very apparent, with material here reaching heights of almost 10 au above the plane. The retrograde disc is slightly less warped, but does not extend out as far. The halo material shows up very clearly as a ring, instead of a continuous shell covering all angles. There is a small amount of material

perpendicular to the main ring only at very high z , the fourth population visible in Figure 7. The warp lies along the 30° - 210° line, as illustrated in the lefthand panel in Figure 11, but the line of sight at around 160° still intercepts a large amount of perturbed coplanar disc material, a good 5 au above the plane of the binary’s orbit. Figure 12 shows similar plots for the other two orbital cases for the azimuthal segment containing the line of sight. In the high eccentricity case of orbit III, almost no material is intercepted, while in the low eccentricity orbit I simulation far more prograde and retrograde material remains, making either this or orbit II the most likely orbital configurations if a warped planetesimal disc and associated dust is the cause of the observed extinction.

Over the length of the simulation, the warp precesses with a timescale equal to twice that of the secular period of the stars, following almost perpendicular to the circulation of the line of intersection of the two stellar orbits. The extent of the warp in fact decreases as the mutual inclination between the stars increases (since the orbit is retrograde the higher the inclination the closer the two planes). The non-symmetrical distribution seen in Figure 11 persists, with one side usually greater in height than the other. The warp is not a short term feature, and the system will persist in its current configuration for some time, so if dust follows the planetesimal distribution it is very likely the extinction is indeed caused by the warp in the disc. It should also be noted that the warped material remains after an additional Myr, and is not slowly eroded away.

The azimuthal particle distribution shown in the right hand panel of Figure 11 shows that the two discs are not skewed in any particular direction, but that the halo is aligned along the minor axis of the inner binary’s orbit. In fact, it remains aligned at this angle over the entire simulation. The material in this halo is seen in projection in the right most panel of Figure 5 as the two clumps discussed earlier. As this material follows the pericentre of the inner orbit, which precesses on the secular time scale, it will not intercept the line of sight for some time and is unlikely to be related to the observed variability and extinction.

An important final question raised by Prato et al. (2001) is the lack of a similar circumbinary disc around the other binary A. As the eccentricity and mass ratio of this pair are both smaller, a disc should be more likely here. In fact, the empirical criteria place the stable zone from around 3 au to 11, 8 and 7 au for orbits I, II and III respectively. A preliminary simulation taking A as a single star confirms this greater stability, so the question still remains as to why

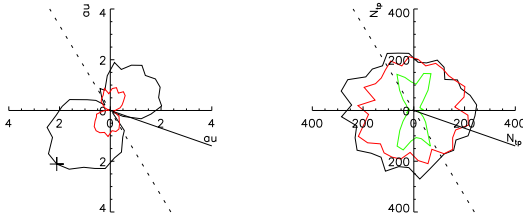


Figure 11. The azimuthal distribution of particles for the simulation using orbit II. The left hand panel shows a polar plot of the warp in the prograde (black) and retrograde (red) discs. The halo is not a disc with respect to this plane so not plotted. The average height away from the plane of the inner binary is shown as a function of azimuthal angle, increasing anticlockwise from the horizontal axis, and the periastron of the inner binary is at 0° . The line of sight is shown as a solid line and the line of intersection of the two orbits as a dashed line (the rising node is towards the bottom right). A plus marks the side of the warp that is above the plane. The right hand panel shows a polar plot of the number of particles in each 10° angle bin. Red and black are as before and the halo is now also plotted in green.

there is no observed disc here. It is possible that the inclination of this binary’s orbit places it so that no planetesimals can remain stable, and if so this would provide limits on the orbit of this stellar pair. Another alternative if there is indeed a disc of stable planetesimals here is that it is far less dusty and so unobserved.

4 CONCLUSION

Dynamical simulations of a planetesimal population in the debris disc around the Bab stellar pair in HD 98800 have been run. By studying a wide range of inclinations, three distinct stable populations have been identified. These are a prograde disc, a retrograde disc and a high inclination halo. The radial profiles of each component are different and distinct. The discs both have large radial gaps, caused presumably by overlapping resonances from the stellar orbits. The radial extent of the discs are summarised in Table 5 but are generally from 3 to 15 au for all three orbits, with gaps at around 4.5 au and 8 au.

The line of sight can currently pass through slightly warped material in the prograde disc, and this would account for the observed extinction and variability if the dust distribution followed the planetesimals. However, this alignment with the line of sight effectively only occurs for the I and II orbits (with eccentricities of 0.3 and 0.5 respectively), which would rule out the higher eccentricity case ($e = 0.6$) as a possible orbit for the outer star.

The radial profile is complex, and illustrates that, for discs in multiple systems, dynamical effects purely due to the stars are very important. Indeed, if most triple stars are within the limit for resonance overlap to sculpt the stability zone, then this has large consequences for debris discs and planet formation in such systems.

The simulation results here can be compared to other models of the system and estimates of the dust distribution. Indeed, as previously mentioned, comparisons to observations of the dust could place constraints on the physical processes occurring in the circumbinary disc. The bulk of the dynamically stable planetesimals are between 5 and 7 au. This matches up well with the prediction of Koerner et al. (2000) of a ring outwards from 5 au. The model of Prato et al. (2001) places the disc from 2 to 5 au, which, apart from the ring around 4.5 au, is unstable here. Furlan et al.

(2007) suggest an inner ring at 2 au and a thicker puffed up component at 5.9 au, the only model to predict gaps and similar to the prograde discs here. The later of these components matches up to the bulk of the material here, and there is indeed an inner ring seen, just further out at 4 au. Prato et al. (2001) estimate the height of the disc as 1 au, and Furlan et al. (2007) as 0.75 au. However, here material in the prograde planetesimal disc is not only warped but very flared, reaching heights of 5 to 10 au. This is an important dynamical feature that should be taken into account in models of the observations. Although roughly agreeing in location, these models do not have enough detail as yet to further compare to the planetesimals.

The dynamical model of Akeson et al. (2007) finds stability from 3 to 10 au, which does not match up that well to the limits here, and in fact their resulting disc has a very different geometry. Their model uses different orbital parameters for the stellar system, most notably a different mutual inclination – as their aim is not to reproduce the current configuration but to look at the general morphological structure of debris discs in highly inclined triple star systems. They also find that the line of sight can intercept a warp in the disc, but due to the different geometry it crosses at a different point and at the maximum warp in the disc, whereas here the warp is only marginally orientated towards the line of sight. It is in fact material in the sparser populated outer regions of the prograde disc that intercepts the line of sight here, from 8 to 15 au, which is a region that in a coplanar stellar system is predicted to be unstable.

The possible dynamical reason for the high infrared excess already mentioned in the Introduction is a close pericentre passage of the A binary stirring up planetesimals and resulting in high collision rates. Since the binary’s period is about 300 years, many such pericentre passages have occurred, and by the end of the simulations the particles appear very stable with regards to this. For example, there appears to be no periodic increase in planetesimal eccentricities as the outer star passes close to the disc. There is, however, another feature that may cause higher than normal collision rates. The extent of the flare and warp in the extended disc decreases as the acute angle between the stellar orbits decreases (and the mutual inclination increases). As this occurs, planetesimals that have been spread out in inclination are now packed into less space. This is likely to result in an increased number of collisions and is particularly relevant as the current stellar configuration is such that mutual inclination is large and the disc is near its narrowest point. However, modelling including collisions is needed to quantify this effect.

The stable high inclination particles in the halo are curious from a dynamical perspective. The Kozai mechanism (Kozai 1962) might be expected to remove such particles very quickly – however these particles do not seem subject to this. It is possible that they are in fact an artifact of the numerical method, but checks with a standard Bulirsch-Stoer integrator (Press et al. 1989) and the similar observation in simulations of GG Tau discount this. The high stellar inclinations involved in the system may be one explanation, but it is worth looking at the stability should one of the binaries be removed. If the outer star is not present, a sharp inner disc edge is seen at around 4 au for all inclinations, with all particles outwards from this remaining stable. If the inner binary is approximated as a single star instead, then a reasonably sharp outer edge is seen at around 7 to 10 au, for the lower inclinations only. The near polar inclinations in this case are now unstable. The high inclination particles are within this region which must be shaped by the combined perturbations from both stellar orbits, so are in a new regime of dynamical behaviour. The mechanism stabilising these particles, as

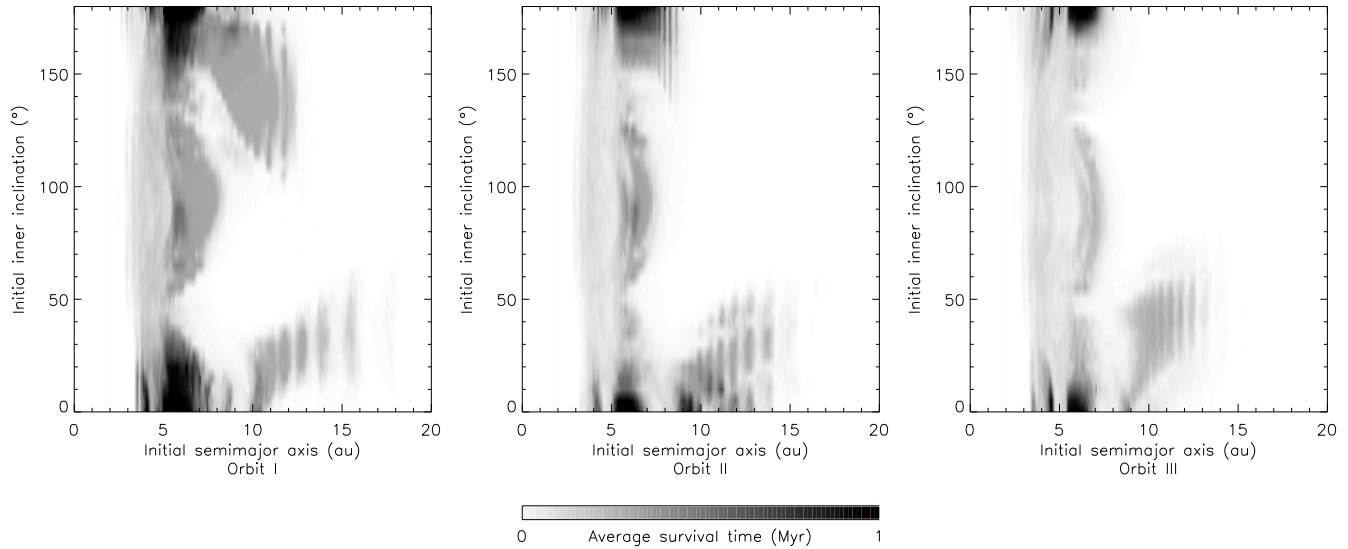


Figure 9. Stability maps comparing the results from the three simulations using orbits I, II and III. The average survival time is shown as a function of initial semimajor axis and inner inclination, with black indicating all particles starting at a given grid point remained at the end of the simulation through to white indicating the location was very quickly unstable.

well as that stabilising the extended prograde and retrograde discs, is the subject of a future paper.

Some consideration is needed, however, of how such material would form. T Tauri multiple systems are common and believed to form primordially through fragmentation processes, which could result in non-coplanar discs (Bate 2000, Bate et al. 2000). As mentioned, Monin et al. (2006) find a small number of multiple T Tauri systems with misaligned discs in their polarization survey, but suggest that perhaps these are perturbed disc soon to be realigned. So there is some evidence that non-coplanar particle distributions are plausible. It may be possible as well that particles from the disc can be captured into the polar stability region, and certainly a coplanar particle distribution is quickly perturbed to fairly high inclinations.

There is much further work to be done in modelling this system. A model of the planetesimals including collisions, although expected to be a minor effect on the dynamics, would indicate if the rate was currently high and may explain the unusually dusty nature of the system. A model that also included dust and dust collisions, as well as interactions with any gas in the system, would then fully model the system and allow detailed comparisons with the observations. Although not an easy task given the nature of the system it would narrow down the physics and dynamics at work, important to our understanding of this stage of the planetary formation process in multiple star systems.

ACKNOWLEDGEMENTS

We would like to thank Mark Wyatt for bringing this unique system to our attention, and for helpful discussions with him and Ken Rice. We would also like to thank the anonymous referee for helpful comments. PEV acknowledges financial support from the Science and Technology Facilities Council.

REFERENCES

- Akeson, R. L., Rice, W. K. M., Boden, A. F., Sargent, A. I., Carpenter, J. M., & Bryden, G. 2007, *ApJ*, 670, 1240
- Bate, M. R. 2000, *MNRAS*, 314, 33
- Bate, M. R., Bonnell, I. A., Clarke, C. J., Lubow, S. H., Ogilvie, G. I., Pringle, J. E., & Tout, C. A. 2000, *MNRAS*, 317, 773
- Beust, H., & Dutrey, A. 2005, *A&A*, 439, 585
- Beust, H., & Dutrey, A. 2006, *A&A*, 446, 137
- Boden, A. F., et al. 2005, *ApJ*, 635, 442
- Dent, W. R. F., Greaves, J. S., & Coulson, I. M. 2005, *MNRAS*, 359, 663
- Ford, E. B., Kozinsky, B., & Rasio, F. A. 2000, *ApJ*, 535, 385
- Furlan, E., et al. 2007, *ApJ*, 664, 1176
- Guilloteau, S., Dutrey, A., & Simon, M. 1999, *A&A*, 348, 570
- Holman, M. J., & Wiegert, P. A. 1999, *AJ*, 117, 621
- Kastner, J. H., Zuckerman, B., Weintraub, D. A., & Forveille, T. 1997, *Science*, 277, 67
- Koerner, D. W., Jensen, E. L. N., Cruz, K. L., Guild, T. B., & Gultekin, K. 2000, *ApJL*, 533, L37
- Kozai, Y. 1962, *AJ*, 67, 591
- Lagrange, A.-M., Backman, D. E., & Artymowicz, P. 2000, *Protostars and Planets IV*, 639
- Low, F. J., Smith, P. S., Werner, M., Chen, C., Krause, V., Jura, M., & Hines, D. C. 2005, *ApJ*, 631, 1170
- Monin, J.-L., Ménard, F., & Peretto, N. 2006, *A&A*, 446, 201
- Prato, L., et al. 2001, *ApJ*, 549, 590
- Press, W. H., Flannery, B. P., Teukolsky, S. A., & Vetterling, W. T. 1989, Cambridge: University Press, 1989
- Skemer, A., Close, L., Hinz, P., Hoffmann, W., Kenworthy, M., & Miller, D. 2007, *ArXiv e-prints*, 712, arXiv:0712.1595
- Soderblom, D. R., et al. 1998, *ApJ*, 498, 385
- Smart, W. M. 1953, London, New York, Longmans, Green [1953], pp205
- Tokovinin, A. A. 1999, *Astronomy Letters*, 25, 669
- Torres, G., Stefanik, R. P., Latham, D. W., & Mazeh, T. 1995, *ApJ*, 452, 870

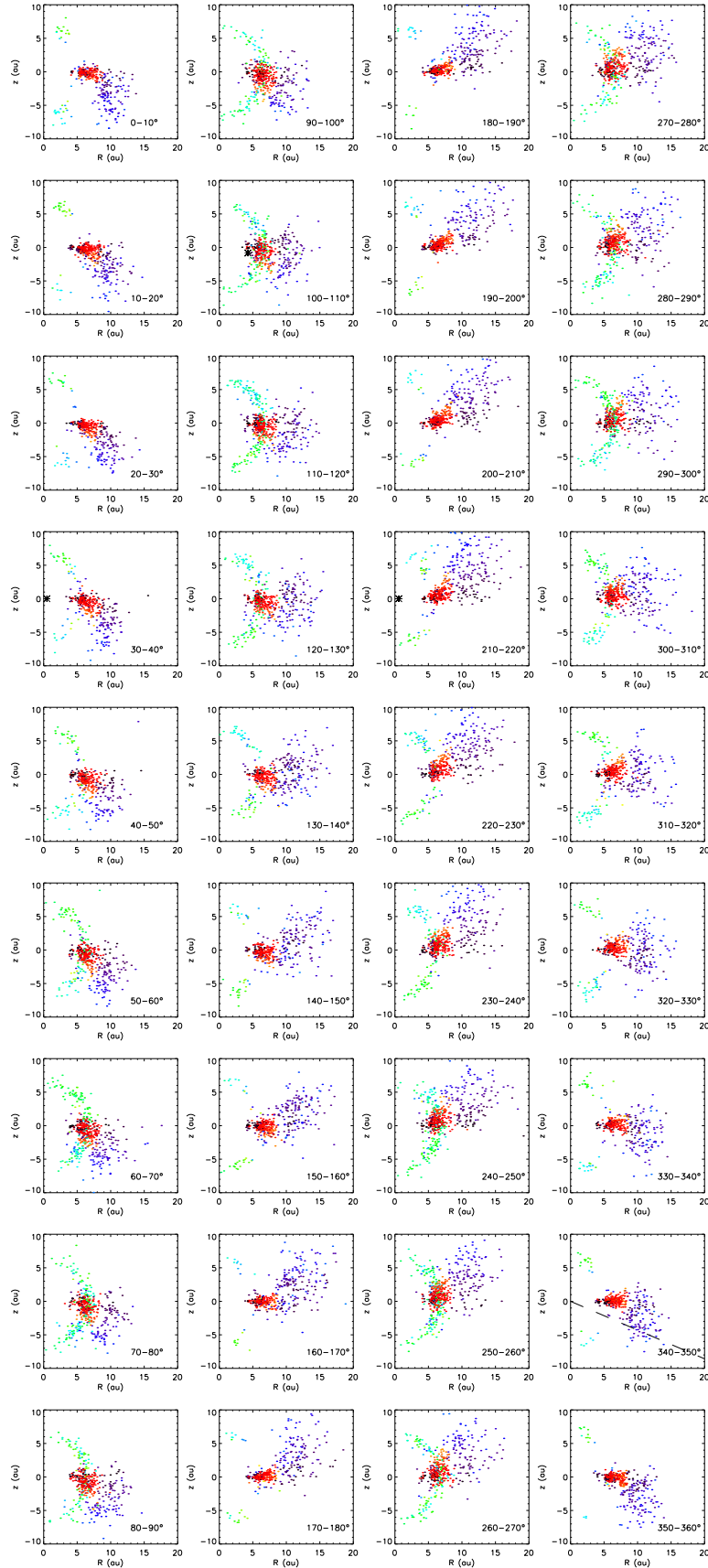


Figure 10. The azimuthal distribution of material for the simulation using orbit II. The panels show the radial distance within the plane of the inner binary and the height above it in segments of 10° . The periastron of the inner binary is at 0° . The stellar positions are overplotted with the outer star shown reduced by a factor of ten, and the line of sight shown as a dashed line. The test particle colour indicates current inner inclination, as in Figure 6.

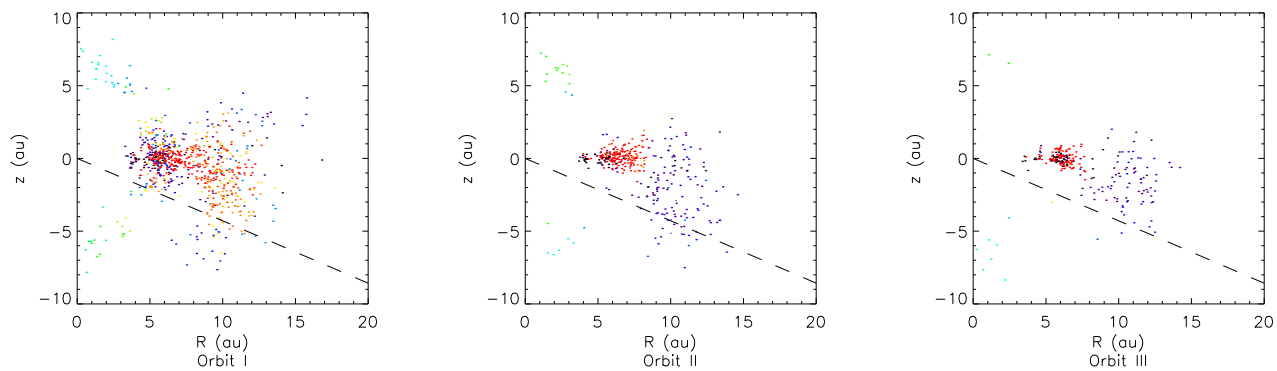


Figure 12. The material intercepting the line of sight in all three simulations. As for Figure 10 radial distance within the plane and height above it is shown with plot points colour-coded to initial inclination. Here however only the segment near the line of sight has been shown for each simulation.

Verrier, P. E., & Evans, N. W. 2007, *MNRAS*, 382, 1432
 Wyatt, M. C., Smith, R., Greaves, J. S., Beichman, C. A., Bryden,
 G., & Lisse, C. M. 2007, *ApJ*, 658, 569